THE JOURNAL OF BIOLOGICAL CHEMISTRY VOL. 282, NO. 14, pp. 10263–10271, April 6, 2007

Kinetic Characterization of the Disulfide Bond-forming Enzyme DsbB*[S]

Received for publication, December 18, 2006, and in revised form, January 5, 2007 Published, JBC Papers in Press, January 31, 2007, DOI 10.1074/jbc.M611541200

Timothy L. Tapley[‡§], Timo Eichner[‡1], Stefan Gleiter[‡2], David P. Ballou[¶], and James C. A. Bardwell[‡§3]

From the [‡]Department of Molecular, Cellular and Developmental Biology, University of Michigan, Ann Arbor Michigan 48109 and [§]Howard Hughes Medical Institute, [¶]Department of Biological Chemistry, University of Michigan, Ann Arbor, Michigan 48109

DsbB is an integral membrane protein responsible for the *de novo* synthesis of disulfide bonds in *Escherichia coli* and many other prokaryotes. In the process of transferring electrons from DsbA to a tightly bound ubiquinone cofactor, DsbB undergoes an unusual spectral transition at ~510 nm. We have utilized this spectral transition to study the kinetic cycle of DsbB in detail using stopped flow methods. We show that upon mixing of $DsbB_{ox}$ and $DsbA_{red}$, there is a rapid increase in absorbance at 510 nm (giving rise to a purple solution), followed by two slower decay phases. The rate of the initial phase is highly dependent upon DsbA concentration ($k_1 \sim 5 \times 10^5\ M^{-1}\ s^{-1}$), suggesting this phase reflects the rate of DsbA binding. The rates of the subsequent decay phases are independent of DsbA concentration ($k_2 \sim 2\ s^{-1}$; $k_3 \sim 0.3\ s^{-1}$), indicative of intramolecular reaction steps. Absorbance measurements at 275 nm suggest that k_2 and k_3 are associated with steps of quinone reduction. The rate of DsbA oxidation was found to be the same as the rate of quinone reduction, suggestive of a highly concerted reaction. The concerted nature of the reaction may explain why previous efforts to dissect the reaction mechanism of DsbB by examining individual pairs of cysteines yielded seemingly paradoxical results. Order of mixing experiments showed that the quinone must be pre-bound to DsbB to observe the purple intermediate as well as for efficient quinone reduction. These results are consistent with a kinetic model for DsbB action in which DsbA binding is followed by a rapid disulfide exchange event. This is followed by quinone reduction, which is rate-limiting in the overall reaction cycle.

Disulfide bonds are post-translational modifications that play vital roles in the folding, stability, and activity of numerous secreted proteins. In the *Escherichia coli* periplasm, disulfide bond formation is catalyzed by the DsbA/DsbB system (for reviews see Refs. 1 and 2). DsbA donates its disulfide bond directly to substrate proteins (3, 4), and to remain catalytically active, DsbA must be reoxidized by an electron acceptor. This role is filled by the enzyme DsbB, which catalyzes the *de novo* formation of disulfide bonds using the oxidizing power of a bound ubiquinone cofactor, which in turn links disulfide bond formation to the electron transport chain (5–9). Although disulfide exchange reactions have been well studied in many systems, much less is known about how they are formed *de novo*. Because DsbB is the primary source of disulfides in the cell, it is of great interest to elucidate its catalytic mechanism.

In the process of transferring electrons from DsbA to ubiquinone, DsbB undergoes a spectral transition to a purple species ($\lambda_{max} \sim 510$ nm). This was first suggested to be due to the formation of a quinhydrone, a stacked ring system consisting of one oxidized and one reduced quinone molecule (10). More recent studies support an alternative explanation in which the Cys^{44} thiolate of DsbB is involved in a charge transfer complex with a DsbB-bound ubiquinone (11, 12). This was supported by the observation that in a DsbB mutant, which only contains only one cysteine (Cys^{44}), a stable purple color is observed. This purple color is independent of DsbA, but it requires quinone. Although the purple intermediate of DsbB is associated with a free Cys^{44}, it is likely that subsequent steps of the reaction, namely the regeneration of an oxidized ubiquinone on DsbB, involve a quinhydrone-like complex.

An intriguing and controversial aspect of the DsbA/DsbB system is the paradoxical redox potentials of the components involved. DsbA contains the most oxidizing disulfide known, with a standard redox potential of −122 mV (13). DsbB contains two essential cysteine pairs, both of which have standard redox potentials that are substantially more reducing than that of DsbA according to most published reports. The Cys^{104}–Cys^{130} pair of DsbB has been shown to react initially with DsbA (14–16), and the redox potential of this cysteine pair has been reported to be anywhere from −284 to −186 mV (17–20). (See Fig. 1 for an overview of the proposed flow of electrons from DsbA to DsbB.) Reported redox potentials for the Cys^{41}–Cys^{44} pair, which is close to the quinone-binding site (21), are extremely variable, from −69 mV (17) to −271 mV (20), with a few intermediate values (−207 and −210 mV) reported as well (18, 19). Ubiquinone in solution has a redox potential of +113 mV (22). The midpoint potential for ubiquinone in mitochondrial membranes is reported to be +65 mV (23). Although the redox potential of DsbB-bound ubiquinone has not been determined, it is expected to be substantially more oxidizing than DsbA, and is thus thought to drive the reaction toward the oxidation of DsbA despite the apparent uphill redox gradient through DsbB. The hyd-

* This work was supported by grants from the National Institutes of Health and Howard Hughes Medical Institute (to J. C. B.) and by a grant from the National Institutes of Health (to D. P. B.). The costs of publication of this article were defrayed in part by the payment of page charges. This article must therefore be hereby marked "*advertisement*" in accordance with 18 U.S.C. Section 1734 solely to indicate this fact.

[S] The on-line version of this article (available at http://www.jbc.org) contains supplemental Figs. S1–S3.

[1] Present address: The Astbury Centre for Structural Molecular Biology, University of Leeds, Leeds LS2 9JT, UK.

[2] Present address: Roche Diagnostics GmbH, Penzberg 82377, Germany.

[3] To whom correspondence should be addressed. Tel.: 734-764-8028; E-mail: jbardwel@umich.edu.

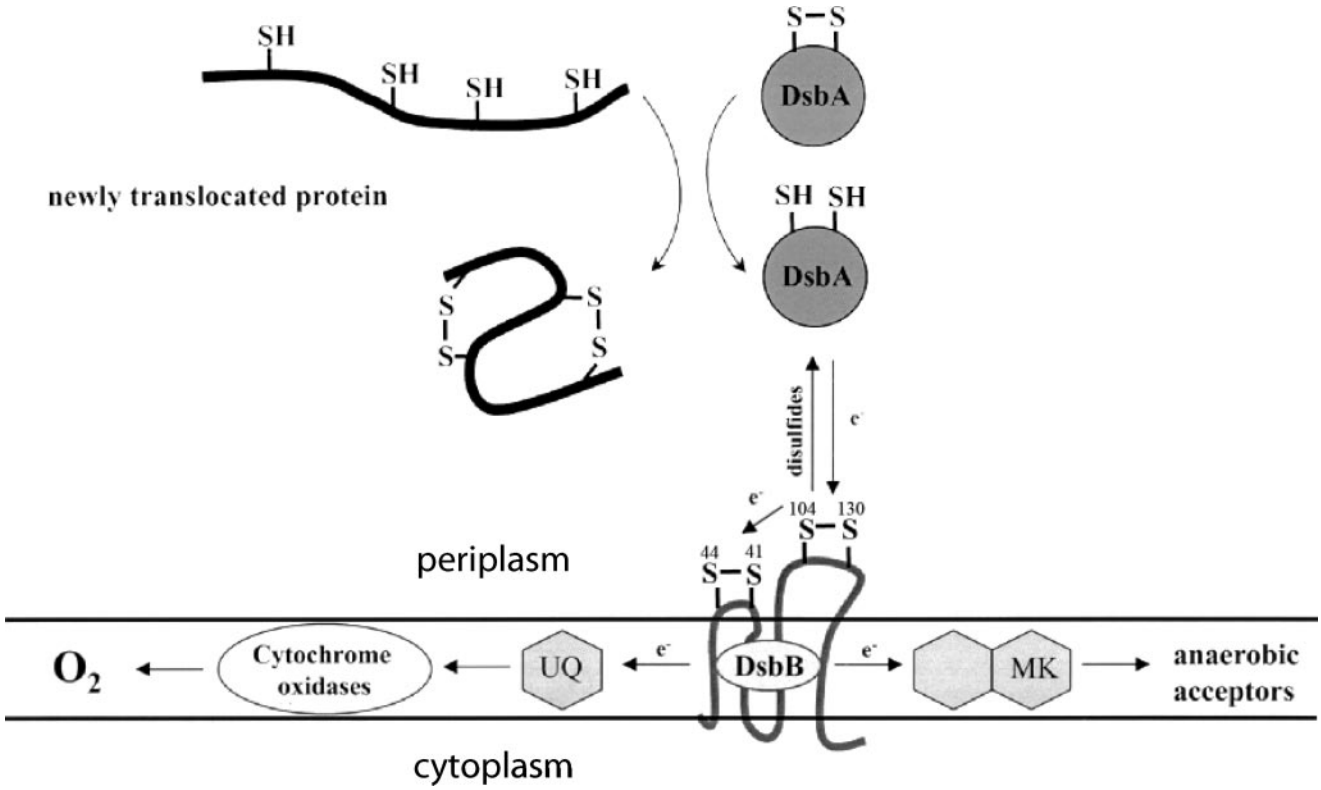

FIGURE 1. **Schematic representation of the flow of electrons from DsbA substrate proteins to DsbA, then to DsbB, and finally to either UQ and the electron transport chain under aerobic conditions or MK under anaerobic conditions.** See text for discussion.

roquinone produced by DsbB is also readily reoxidized by the electron transport chain and O_2, further driving the reaction.

The recently solved crystal structure of a DsbB-DsbA complex has shed some light on the reaction mechanism of DsbB (24). This structure revealed four transmembrane helices that surround the bound ubiquinone cofactor. The head group of the quinone is positioned near the periplasmic membrane interface and is slightly solvent-exposed, whereas the isoprenoid tail, although invisible in the structure, is predicted to project down into the center of the membrane. Most notably, it was observed that Cys^{104}, which is located in a mobile periplasmic loop of DsbB, becomes separated from Cys^{130} upon DsbA binding. This apparently enables Cys^{104} to contact Cys^{41} on the adjacent loop and helps prevent the unproductive backward resolution of the DsbA-DsbB complex. Although this structure represents a milestone in our understanding of the DsbA-DsbB machinery, there remains very limited kinetic data concerning the reactions between these proteins. We have therefore used rapid mixing kinetic measurements to analyze the reaction between DsbA and DsbB. Based on our results we present a kinetic scheme for the DsbB reaction cycle. This study begins to unravel the kinetic mechanism of an enzyme that converts the oxidizing equivalents of quinones to generate disulfide bonds. As such, it serves as the primary source of disulfide bonds in prokaryotes.

EXPERIMENTAL PROCEDURES

Protein Expression and Purification—DsbA and DsbB proteins were expressed and purified essentially according to previously published protocols (5, 7), as were quinone-free and menaquinone-bound DsbB (19, 25). Reduced DsbA was prepared by incubation with 50 mM dithiothreitol for 1 h at room temperature, followed by extensive dialysis against 50 mM sodium phosphate buffer, pH 7, containing 1 mM EDTA. DsbA was confirmed to be in a fully reduced state as judged by reactivity with Ellman's reagent (26).

Stopped Flow Absorbance Measurements—Stopped flow absorbance measurements were performed on Hi-Tech Scientific SF61 instruments equipped with a either a 50-watt halogen lamp (for visible measurements) or a 75-watt xenon lamp (for UV measurements). Experiments were performed at 10 °C in PND buffer (50 mM sodium phosphate, 300 mM NaCl, 0.04% *n*-dodecyl-β-D-maltopyranoside, pH 8.0). Protein concentrations are given in the figure legends. Traces shown are representative of a minimum of six to eight successive shots, and the data for each trace were fit individually. The observed rates for each trace at a given concentration were then averaged, and error bars are shown as one standard deviation.

Stopped Flow Fluorescence Measurements—Stopped flow fluorescence measurements were carried out on a Kintek instrument equipped with a 75-watt xenon lamp. An excitation wavelength of 295 nm (5 nm spectral bandpass) was used in conjunction with a 340-nm cutoff filter for emission. All fluorescence experiments were performed in PND buffer at 25 °C, and additional absorbance measurements (510 nm) were performed at 25 °C for comparison. Traces shown are representative of a minimum of six to eight successive shots, and the data for each trace were fit individually.

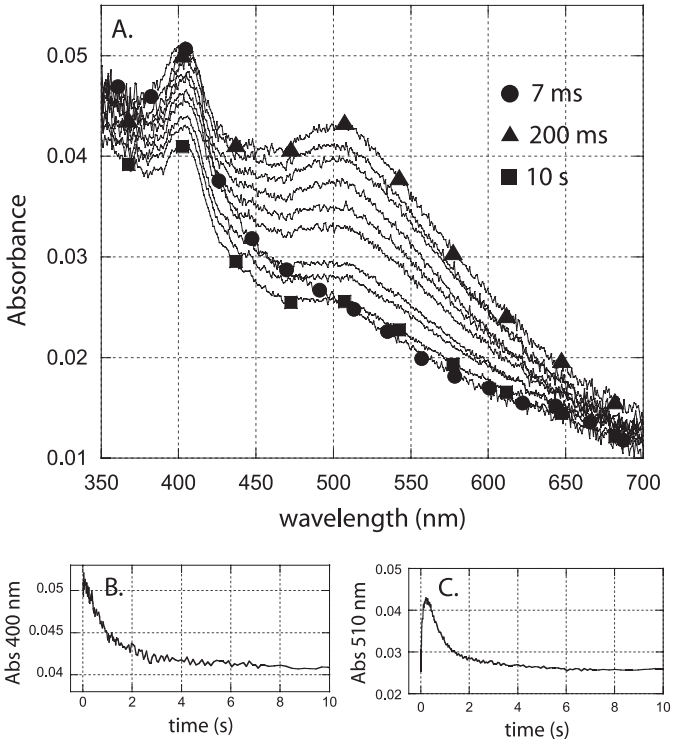

FIGURE 2. **Time resolved spectra of DsbB reaction intermediates.** *A,* spectra were recorded with a photodiode array detector at time intervals from 7 ms to 10 s upon rapid mixing of equimolar $DsbA_{red}$ and $DsbB_{ox}$ (15 μM final concentrations) in PND buffer at 10 °C. Spectra collected at 7 ms (*circles*), 200 ms (*triangles*), and 10 s (*squares*) are marked. *B* and *C* show absorbance changes at 400 and 510 nm (respectively) as a function of time.

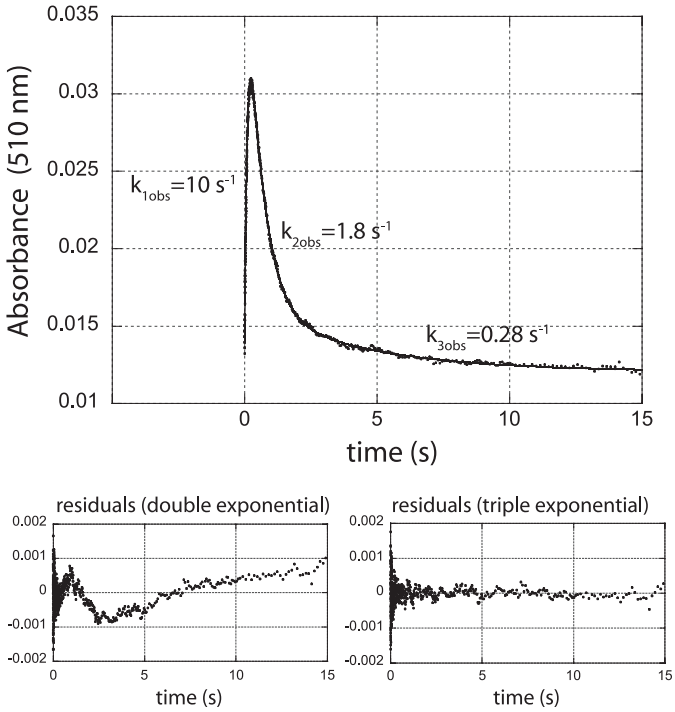

FIGURE 3. **Stopped flow absorbance measurements at 510 nm.** Absorbance changes at 510 nm induced by mixing $DsbA_{red}$ (15 μM final concentration) and $DsbB_{ox}$ (15 μM final concentration) in PND buffer at 10 °C. The data were fit to a triple exponential function; residuals for fits to a double or triple exponential function are shown.

Enzyme-monitored Turnover—Multiple turnover experiments were performed using a HiTech SF61 instrument according to the protocol established by Gibson *et al.* (27). 10 μM DsbB was mixed with 100 μM DsbA and 200 μM quinone (Q1)[4] in PND buffer at 10 °C, and absorbance at 510 nm was monitored over time. The time course of the disappearance of the purple intermediate of DsbB is related to the rate of enzyme turnover, and this trace was used to derive a velocity *versus* [DsbA] plot using program A.

Data Analysis—Curve fitting was performed with Kaleidagraph (Synergy Software) using equations for single, double, and triple exponential functions. Errors are reported as ±1 S.D.

RESULTS AND DISCUSSION

DsbA is critical for catalyzing disulfide bond formation in proteins in the bacterial periplasm, which it accomplishes by directly oxidizing substrate proteins via dithiol-disulfide exchange (3, 4). In order to be maintained in a catalytically active state, reduced DsbA must then be reoxidized by DsbB. It has been shown previously that reduced DsbA initially attacks the Cys^{104}–Cys^{130} disulfide of DsbB (14–16). This binding is followed by a thiol-disulfide exchange reaction with a second disulfide (Cys^{40}–Cys^{44}) of DsbB. The resulting free thiolate anion of Cys^{44} is involved in a charge-transfer complex with the DsbB-bound quinone cofactor to give a characteristic absorbance at ~510 nm (11). We took advantage of this spectral intermediate to study the kinetic mechanism of DsbB. Time-resolved spectra collected by rapid mixing of equimolar concentrations of $DsbA_{red}$ and $DsbB_{ox}$ are shown in Fig. 2*A*. Two notable features become apparent upon analysis of these spectra; first is the rapid increase in absorbance at ~510 nm, which reaches a maximum at ~200 ms and then decays with a slower rate back to approximately the initial level. Second is the absorbance peak at ~400 nm, which does not change substantially during the first 200 ms after mixing but then decays at a rate similar to that of the absorbance decay at 510 nm (see Fig. 2, *B* and *C,* for kinetic traces of absorbance changes at 400 and 510 nm derived from the spectra). Ubiquinone has a weak absorbance peak at ~400 nm ($\epsilon \sim 420\ M^{-1}cm^{-1}$) that essentially disappears upon reduction.[5] Reduction of 15 μM DsbB-bound quinone would be expected to cause a decrease in absorbance at 400 nm of 0.0063, and the observed absorbance change was ~0.01. Therefore, the simplest interpretation of the data presented in Fig. 2 is that the rise in absorbance at 510 nm reflects the generation of the DsbB Cys^{44}-quinone charge-transfer intermediate, and the subsequent decay (at both 400 and 510 nm) corresponds to quinone reduction. Note that this overall process is significantly faster than reported in a similar previously published experiment (11). This is most likely because of differences in pH and temperature. It seems likely that *in vivo* (*i.e.* at pH 7 and 37 °C) the process will be even faster.

To obtain more accurate rate constants, we monitored the formation and decay of the purple intermediate of DsbB using

[4] The abbreviations used are: Q1, ubiquinone 1; UQ, ubiquinone; MK, menaquinone; Q8, ubiquinone 8; WT, wild type.

[5] T. Tapley, unpublished data.

single wavelength measurements at 510 nm. A representative trace obtained upon mixing equimolar $DsbA_{red}$ and $DsbB_{ox}$ is shown in Fig. 3*A*. The data do not fit well to a double exponential function (see Fig. 3*B* for residuals). A triple exponential function (see Fig. 3*C* for residuals) yielded an excellent fit, suggesting that the purple intermediate (the Cys^{44}-quinone charge-transfer complex) decays in a two-step process. The absorbance increase is because of the formation of the intermediate at a rate of $10 \pm 0.5\ s^{-1}$ (k_{1obs}), and the decay of this intermediate occurred in two phases of 1.8 ± 0.08 and $0.28 \pm 0.03\ s^{-1}$ (k_{2obs} and k_{3obs}). The amplitudes of the first and second phases are roughly equal and opposite ($\Delta A = 0.045$ and -0.04 respectively), with the third phase comprising only ~10% of the decay phase ($\Delta A = -0.005$).

We performed a series of experiments over a range of DsbA concentrations to determine which rates were associated with the initial reaction(s) with DsbA, as opposed to subsequent intramolecular reaction steps. The traces were fit to triple exponential functions, and the observed rates were plotted against DsbA concentration. As shown in Fig. 4*A*, the rate of formation of the purple intermediate is highly dependent upon DsbA concentration ($k_1 = 5.2 \times 10^5\ M^{-1}\ s^{-1}$). This was somewhat surprising because the purple intermediate is thought to correspond to an interaction between Cys^{44} of DsbB and the bound ubiquinone (11, 12). DsbA, however, has been shown to initially cleave the Cys^{104}–Cys^{130} disulfide of DsbB (14–16) (see Fig. 1), which in turn triggers a thiol-disulfide exchange that results in the cleavage of the Cys^{40}–Cys^{44} disulfide of DsbB (leaving a free thiolate at position 44). Therefore, the purple intermediate forms only after an intramolecular thiol-disulfide exchange reaction. Because it is an intramolecular reaction, this step is expected be independent of DsbA concentration unless the rate of DsbA binding is slower than the intramolecular thiol-disulfide exchange reaction. The results in Fig. 4*A* are therefore suggestive of a thiol-disulfide exchange event that is much faster ($\gg 50\ s^{-1}$) than the rate of DsbA binding and formation of its mixed disulfide under our experimental conditions. This rapid disulfide exchange reaction enables tight coupling of the process to the reduction of ubiquinone. The dissociation of DsbA occurs at a much slower rate (k_{-1}, as given by the *y*-intercept of Fig. 4*A*, ~$1.6\ s^{-1}$).

Unlike the absorbance increase at 510 nm, the two subsequent decay phases show little dependence on DsbA concentration (see Fig. 4, *B* and *C*), indicating that these are intramolecular reaction steps. The major decay phase (k_2)occurs with a rate of ~$2\ s^{-1}$ over the full range of DsbA concentrations tested, whereas the minor decay (k_3) occurred at a rate of $0.3\ s^{-1}$.

The results presented in Fig. 2 suggest that the absorbance decay at 410 nm (and the corresponding decay at 510 nm) corresponds to the rate(s) of quinone reduction. The observation that these rates (k_2 and k_3) do not depend on DsbA concentration is also consistent with this hypothesis. To further test this, we utilized the absorbance properties of ubiquinone, which absorbs strongly at 275 nm in the oxidized state, but is dramatically decreased upon reduction ($\Delta\epsilon_{275} = -12{,}250\ M^{-1}\ cm^{-1}$). This gives us a robust and reliable spectroscopic signal by which to monitor the rate of quinone reduction. We therefore performed stopped flow absorbance measurements at 275 nm under the same conditions used in Fig. 3. As expected, the absorbance at 275 nm decreases upon mixing DsbA and DsbB (Fig. 5). This trace is well described by a double exponential function (see Fig. 5, *B* and *C*, for residuals for single and double exponential fits), with observed rates of ~1.5 and $0.23\ s^{-1}$. These rates are very similar to the rates of decay of the purple intermediate, indicating that the rates of absorbance decay at 510 nm indeed correspond to the rate(s) of quinone reduction. As was observed for absorbance measurements at 510 nm, the magnitude of the first phase is dominant (0.045) and followed by a smaller minor decay phase (0.015). Based on the known extinction change at 275 nm between oxidized and reduced ubiquinone, these absorbance changes suggest that ~40% of the bound quinone is reduced in this process. This may reflect

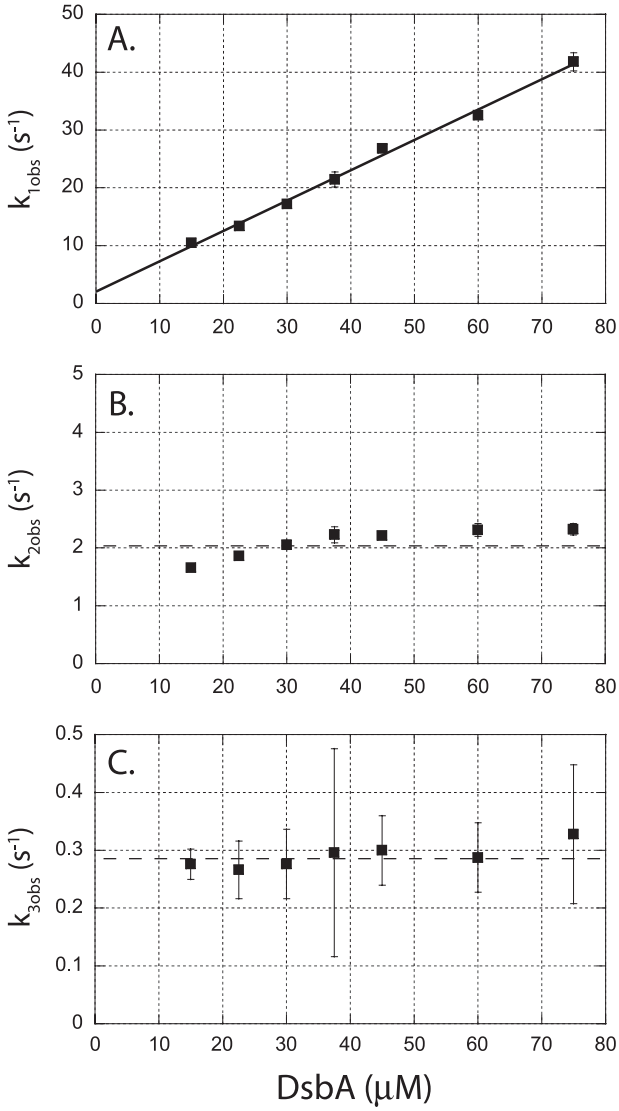

FIGURE 4. **Dependence of $k_{1,obs}$, $k_{2,obs}$ and $k_{3,obs}$ on DsbA concentration.** Stopped flow absorbance measurements (510 nm) were conducted as in Fig. 3 but over a range of DsbA concentrations from 15 to 75 μM. The data were fit to triple exponential functions, and the observed rates were plotted *versus* DsbA. The *line* in *A* represents a least squares linear regression fit to the data and yields a slope of $5.2 \times 10^5\ M^{-1}\ s^{-1}$ and a *y*-intercept of $1.6\ s^{-1}$. The *dashed lines* in *B* and *C* represent average values of $k_{2,obs}$ ($2.1 \pm 0.24\ s^{-1}$) and $k_{3,obs}$ ($0.29 \pm 0.020\ s^{-1}$).

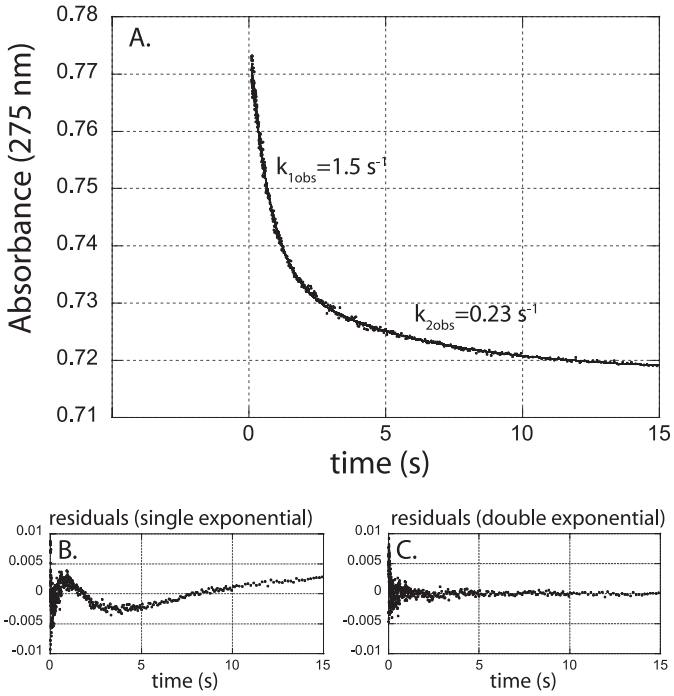

FIGURE 5. **Stopped flow absorbance measurements at 275 nm.** *A*, absorbance changes at 275 nm were induced by mixing $DsbA_{red}$ (15 μM final concentration) and $DsbB_{ox}$ (15 μM final concentration) in PND buffer at 10 °C. The data were fit to a double exponential function; residuals for fits to single (*B*) or double (*C*) exponential functions are shown.

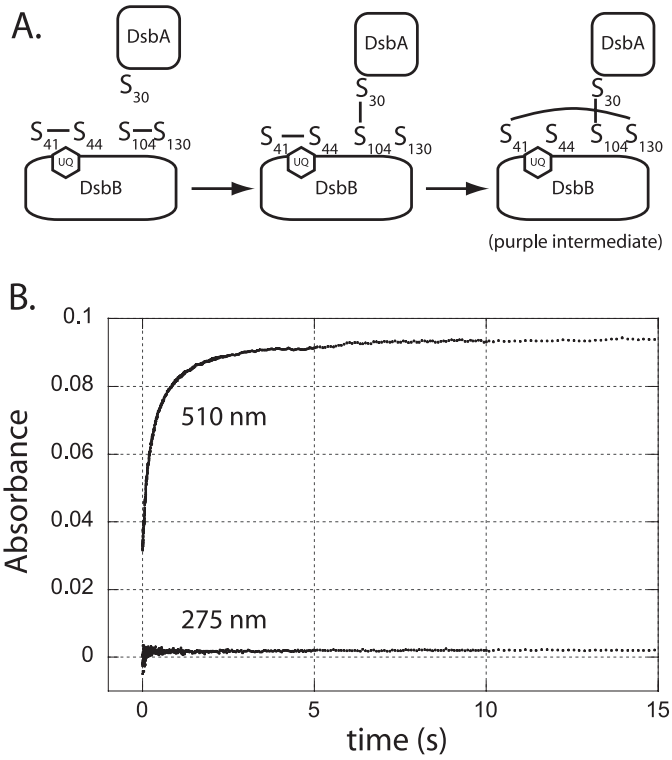

FIGURE 6. *A,* diagram of the interaction between DsbA(C33S) and DsbB. *B,* kinetics of absorbance changes at 510 and 275 nm induced by mixing 15 μM DsbA(C33S) and 15 μM DsbB (final concentrations) in PND buffer at 10 °C. Absorbance at 275 nm is offset by ~0.7.

the presence of a fraction of inactive enzyme in our preparations, or the extinction coefficient of DsbB-bound quinone is different from that of free quinone in aqueous buffer. More complete kinetic analysis (as in Fig. 4) was not be carried out because of the high absorbance at 275 nm at high protein concentrations, although experiments conducted with 75 μM DsbA suggested that the rates of absorbance decay at 275 nm (~1.6 and 0.25 s^{-1}) are independent of DsbA concentration (data not shown), as was observed for absorbance measurements at 510 nm. Therefore, the signal observed at 275 nm, which we interpret as a decrease in absorbance because of quinone reduction, reflects intramolecular reaction steps. This suggests that quinone reduction does not occur via direct interaction with DsbA, which is in line with the current model for DsbB action.

The results presented thus far suggest that the decay of absorbance at 510 and 275 nm is because of reduction of the DsbB-bound quinone. To exclude the possibility that changes in protein absorbance also contribute significantly to the observed signal at 275 nm, we performed similar experiments with a DsbA mutant (C33S) that lacks one of the two essential active site cysteines. As such, it cannot complete a dithiol-disulfide exchange reaction with DsbB and therefore does not support quinone reduction. It instead forms a stable mixed disulfide complex that is able to induce a stable purple intermediate form of DsbB (11), as diagramed in Fig. 6*A*. As shown in Fig. 6*B*, rapid mixing of equimolar amounts of DsbB with DsbA(C33S) resulted in a stable accumulation of the purple intermediate as evidenced by an absorbance increase at 510 nm. In contrast to experiments with WT DsbA, no subsequent absorbance decay was observed. In addition, analysis of absorbance changes at 275 nm showed that there was no decrease in signal upon mixing DsbB and DsbA(C33S) (Fig. 6*B*, *lower trace*). This confirms that changes in protein absorbance (at least up to the stage of a mixed disulfide complex between DsbB and DsbA) are not responsible for the observed absorbance decreases at 275 nm in experiments with WT DsbA but that the observed signal change (*i.e.* in Fig. 5*A*) is indeed because of quinone reduction.

Order of Mixing Experiments—As purified, DsbB contains ~1 molecule of tightly bound ubiquinone 8 (Q8). In previously published studies, it was unclear at which point the quinone begins to participate in the reaction. It has been proposed that DsbB oxidizes the DsbA active site cysteine pair and that DsbB is subsequently oxidized by ubiquinone. However, it is difficult to distinguish precisely when the quinone cofactor becomes an important reaction component in the overall process. To address this issue we purified a quinone-free form of DsbB (designated DsbBΔUQ) and performed order of mixing experiments. In one case we rapidly mixed DsbBΔUQ that had been pre-equilibrated with Q1 and with DsbA, and in the next experiment we mixed DsbBΔUQ with a solution containing DsbA and Q1. When preincubated DsbBΔUQ and Q1 were rapidly mixed with DsbA, a rapid increase in absorbance at 510 nm followed by a slower decay phase was observed (Fig. 7*A*), similar to results observed in previous experiments. The rate of absorbance increase was relatively unaffected by replacement of Q8 with Q1, implying that the rate of DsbA binding and the subsequent thiol-disulfide exchange reaction are not strongly dependent on the nature of the quinone cofactor. The rate of decay of the absorbance signal at 510 nm (*i.e.* the rate of qui-

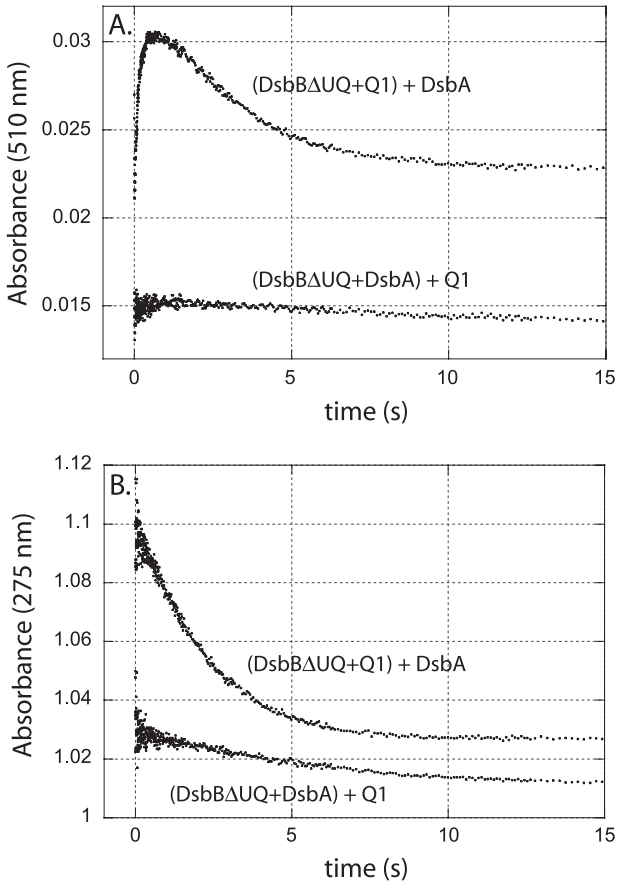

FIGURE 7. **Order of mixing experiments.** *A*, absorbance changes at 510 nm induced by mixing either pre-equilibrated DsbBΔUQ+Q1 with DsbA or pre-equilibrated DsbBΔUQ+DsbA with Q1 (each to final concentrations of 15 μM) in PND buffer at 10 °C. *B*, absorbance changes at 275 nm using the same protocol as in *A*.

none reduction), however, is ~6-fold slower than when Q8 is present (compare Fig. 7*A* with Fig. 3). We have shown that the absorbance decay at 510 nm reflects the rate of quinone reduction. Thus, it appears that the isoprenoid tail of Q8 may help to optimally position the quinone within the active site of DsbB, making quinones with shorter lipid tails less than ideal cofactors for DsbB.

We next tested whether the formation of the purple intermediate is dependent on a quinone being pre-bound to DsbB. When we preincubated DsbBΔUQ and DsbA, and then mixed with Q1, we did not observe any appreciable absorbance changes at 510 nm (Fig. 7*A*, *lower trace*). Absorbance changes at 275 nm (Fig. 7*B*) echoed the results obtained at 510 nm; preincubation of DsbBΔUQ and DsbA followed by mixing with Q1 led to very little signal.

Taken together, these results suggest that a pre-bound quinone on DsbB is required for formation of the purple intermediate of DsbB (transient absorbance at 510 nm) as well as for efficient quinone reduction (absorbance decrease at 275 nm). There are several reasons why this could be the case. First, the entire reaction may be a highly concerted process that requires quinone to be in place before disulfide exchange between DsbA and DsbB occurs, and mixing DsbA and DsbB in the absence of quinone could lead to an off pathway reaction. Alternatively, DsbA binding may occlude the quinone-binding site and thereby prevent quinone binding. This seems very unlikely, however, based on the recently solved structure of the DsbA-DsbB complex (24). Finally, Q1 binding to DsbB may be very slow. This also seems unlikely however, and we have performed steady-state and stopped flow fluorescence experiments that suggested, to the contrary, that Q1 binding is extremely fast (data not shown). Therefore, we are drawn back to our initial interpretation that the reaction between DsbA, DsbB, and ubiquinone is a highly concerted process. The highly concerted nature of the reaction explains why previous attempts to dissect the reaction mechanism of DsbB by looking at individual cysteine pairs yielded seemingly paradoxical results. The results presented in Fig. 7 clearly demonstrate that in order for the reaction to proceed efficiently, DsbB must have a quinone bound prior to DsbA binding. The high affinity of the natural UQ8 cofactor would ensure that this requirement is met *in vivo*.

This tight association between DsbB and UQ8 raises the question of how reduced quinone (quinol) is oxidized to regenerate a catalytically competent DsbB. We see two possible solutions. First, the quinol form may bind with a weaker affinity and upon reduction may dissociate from DsbB to be reoxidized by cytochrome oxidases. This would be followed by a "fresh" (*i.e.* oxidized) quinone binding DsbB. Alternatively, the quinol could remain tightly bound to DsbB and be reoxidized by a second quinone via a quinhydrone complex. The fact that the quinone remains tightly bound in nearly stoichiometric amounts leads us to favor the second model. We are currently engaged in studies aimed at distinguishing between these two possibilities.

Stopped Flow Fluorescence Measurements—Reduced DsbA is known to undergo a substantial fluorescence decrease upon oxidation, which is because of quenching of the only fluorescent tryptophan residue (Trp^{76}) by the Cys^{30}–Cys^{33} disulfide bond (28). DsbB exhibits a large increase in fluorescence upon reduction, and it is has been proposed that this effect may be because of removal of quenching by quinone as it is reduced (19). Thus, the fluorescence changes upon mixing reduced DsbA and oxidized DsbB are because of changes from both proteins. We found that the fluorescence increase because of DsbB reduction is greater than the fluorescence decrease upon DsbA oxidation, so the net fluorescence signal upon mixing $DsbA_{red}$ and $DsbB_{ox}$ is a fluorescence increase (see supplemental Fig. 1*A*). In an attempt to dissect the contribution because of DsbB alone, we utilized a mutant form of DsbA in which the fluorescent tryptophan residue is substituted with phenylalanine, resulting in a protein that exhibits almost no intrinsic fluorescence (supplemental Fig. 1*B*). As we expected, when DsbA(W76F) and DsbB were mixed, the fluorescence increase was greater than the corresponding experiment with WT DsbA (supplemental Fig. 1*B*).

We performed stopped flow fluorescence measurements in an attempt to deduce the rate of DsbA oxidation during the reaction cycle. This might be distinguished by an initial decrease in fluorescence before DsbB has reduced the quinone. We found that upon rapid mixing of $DsbA_{red}$ and $DsbB_{ox}$, a three-phase change in tryptophan fluorescence could be observed (Fig. 8*A*). The first phase is a small but significant decrease in fluorescence, followed by a large fluorescence

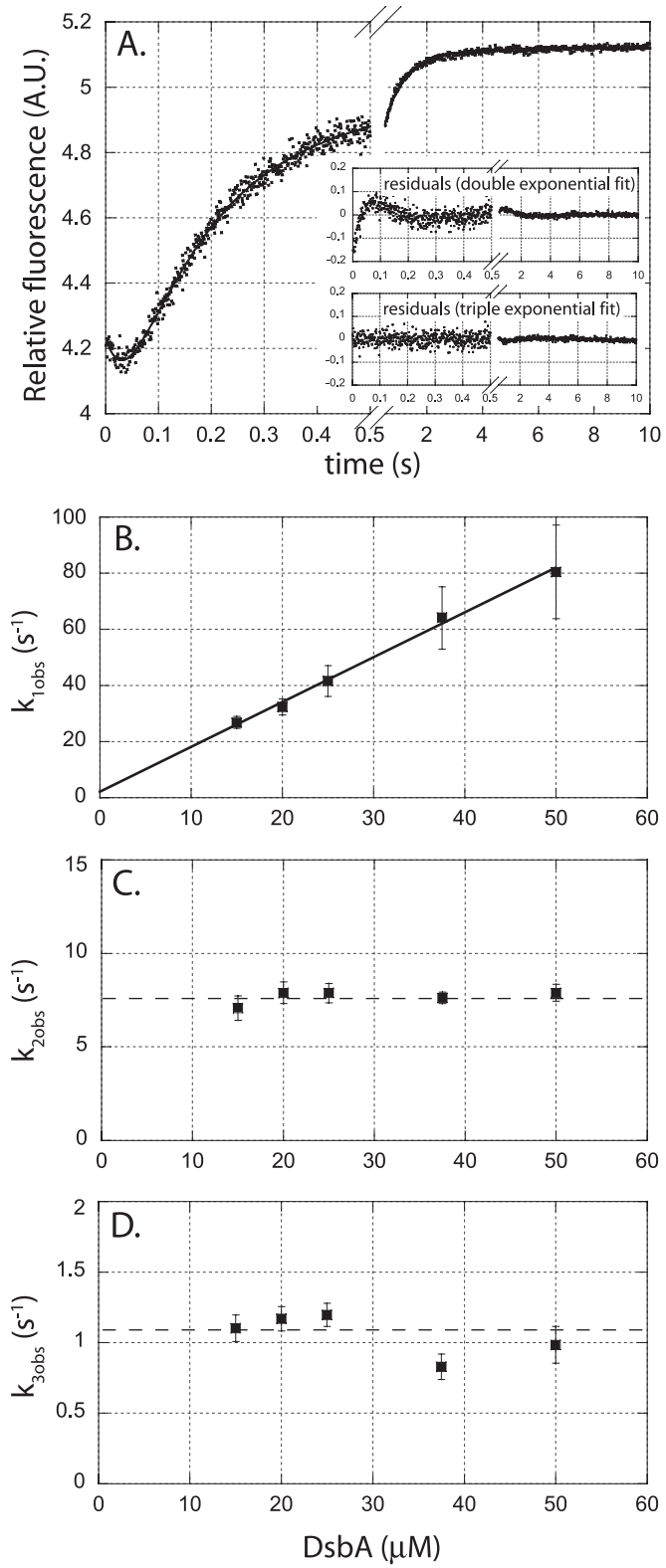

FIGURE 8. **Stopped flow fluorescence measurements.** *A,* kinetic trace of changes in tryptophan fluorescence (ex = 295 nm, em > 340) induced by mixing 5 μM DsbB with 15 μM DsbA (final concentrations) in PND buffer at 25 °C. Data were fit to a triple exponential function, which yielded rates for $k_{1,obs}$, $k_{2,obs}$, and $k_{3,obs}$ of 25, 7.5, and 1.1 s^{-1}, respectively. The *insets* show residuals for double and triple exponential fits. *B–D* show the dependence of $k_{1,obs}$, $k_{2,obs}$, and $k_{3,obs}$ on DsbA concentration. The *line* in *B* represents a least squares linear regression fit to the data and yields a slope of 1.6×10^6 M^{-1} s^{-1} and a *y*-intercept of 2.2 s^{-1}. The *dashed lines* in *C* and *D* represent average values of $k_{2,obs}$ (7.7 ± 0.4 s^{-1}) and $k_{3,obs}$ (1.1 ± 0.2 s^{-1}).

increase, and finally by a slower and smaller increase in fluorescence. Because these experiments were performed under slightly different conditions than the absorbance measurements presented in Figs. 3 and 4 (25 *versus* 10 °C), we performed additional absorbance measurements at 510 nm to compare rates of absorbance *versus* fluorescence changes under identical reaction conditions. We found that all three rates measured in fluorescence experiments correspond almost exactly to the three phases observed in absorbance (510 nm) measurements under the same experimental conditions (supplemental Fig. 2), suggesting that the underlying causes for absorbance and fluorescence changes are the same. Furthermore, stopped flow fluorescence (and absorbance) measurements performed over a range of DsbA concentrations confirmed that the first phase is highly dependent upon DsbA concentration (Fig. 8*B*), whereas the second and third were not (Fig. 8, *C* and *D*). This suggests that the initial small decrease in fluorescence is because of either binding of DsbA or the subsequent (rapid) thiol-disulfide exchange event, which produces the free thiolate of Cys^{44}. A similar experiment in which we mixed DsbB with DsbA(C33S) resulted in a similarly small, monophasic decrease in fluorescence (data not shown), suggesting that this decrease is because of binding of DsbA or because of the formation of the mixed disulfide between DsbA and DsbB, and not because of the oxidation of the Cys^{30}–Cys^{33} disulfide of DsbA. The observation that there are only two remaining phases and these phases correspond almost exactly with the rates of absorbance decreases suggests that DsbA oxidation and quinone reduction occur at the same rate. This is consistent with a highly concerted reaction, as has been suggested previously (29).

We also performed kinetic measurements of fluorescence changes induced upon mixing DsbA(W76F) with DsbB (Fig. S3). Because DsbA(W76F) is nonfluorescent, the entire kinetic trace obtained in this experiment is because of changes in DsbB fluorescence. This trace showed the same general features of the experiment performed with WT DsbA, *i.e.* a very fast small decrease in fluorescence, followed by two phases in which the fluorescence increased. The overall magnitude of the fluorescence increases is larger with DsbA(W76F) because the "negative" contribution due to DsbA oxidation is eliminated. Therefore, we can say with some level of confidence that in the experiments with WT DsbA, the fluorescence decreases because of DsbA oxidation are occurring with the same rates as the fluorescence increases because of DsbB (or more likely because of quinone reduction). This again is suggestive of a highly concerted reaction in which DsbA oxidation and quinone reduction are occurring nearly simultaneously.

Multiple Turnover Experiments—Although the main focus of this study was to characterize DsbB by observing the formation and decay of the Cys^{44}-UQ charge-transfer complex, we also wanted to relate the rates we measured for individual steps of the reaction with the overall rate of reaction (k_{cat}) under similar conditions. We used both a previously described fluorescence-based assay (6) and the enzyme-monitored turnover method described by Gibson *et al.* (27) to determine the steady-state kinetic parameters, K_m and V_{max}. The latter method utilizes the time course of the decay of an enzyme intermediate (in our case, the purple species of DsbB) upon reaction with an excess of

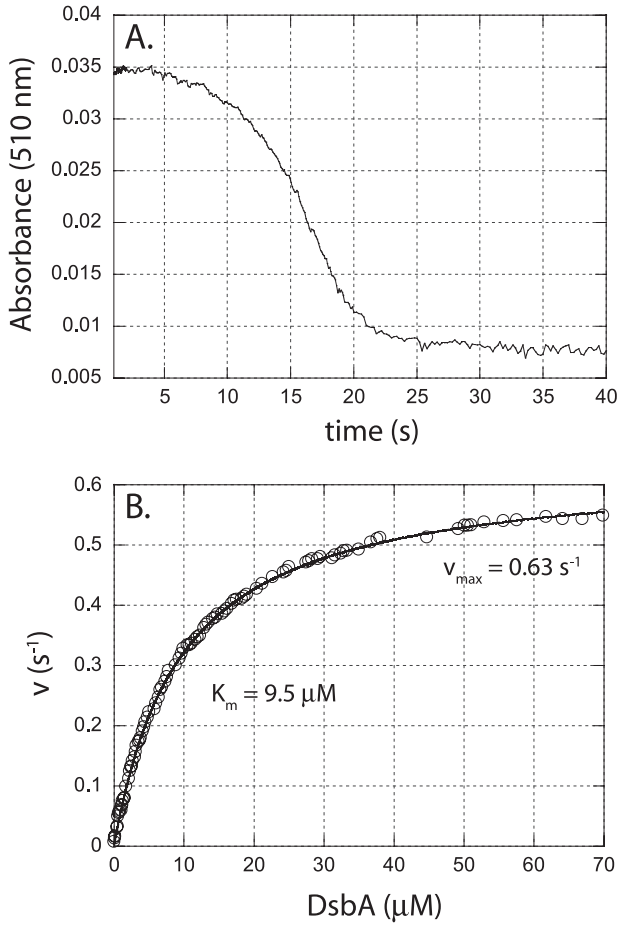

FIGURE 9. **Enzyme monitored turnover.** *A,* absorbance changes at 510 nm induced by mixing 10 μM DsbB, 200 μM Q1, and 100 μM DsbA in PND buffer at 10 °C. This trace was used to derive a *V versus* [S] plot (shown in *B*) using the enzyme-monitored turnover method (27). The *solid line* represents the best fit to a hyperbolic saturation function.

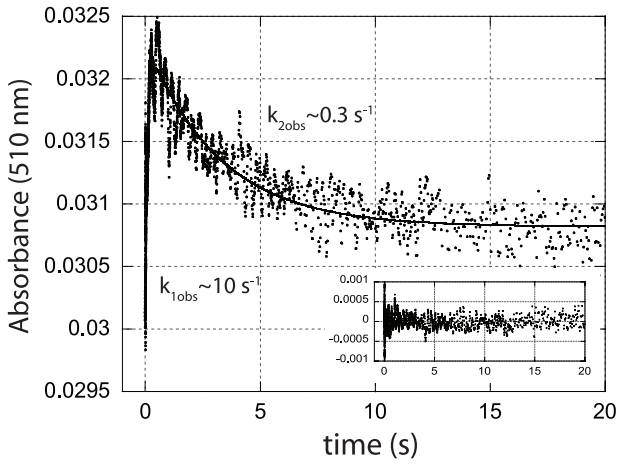

FIGURE 10. **Stopped flow absorbance measurements with menaquinone-bound DsbB.** Absorbance changes at 510 nm induced by mixing DsbA (15 μM final concentration) and DsbB(MK) (15 μM final concentration) in PND buffer at 10 °C. The data were fit to a double exponential function; residuals for the fit to a double exponential function are shown in the *inset.*

substrate to derive a velocity *versus* [substrate] plot. The amount of intermediate present is representative of the amount of DsbB forming product at any given time.

As shown in Fig. 9*A*, mixing 10 μM DsbB with 100 μM DsbA and 200 μM (excess) Q1 leads to a nearly steady level of the purple intermediate for the first few seconds, and this is followed by a decay in the signal as reduced DsbA is consumed and the velocity of turnover decreases. This trace was then used to derive a velocity *versus* [DsbA] plot, which is shown in Fig. 9*B*. This plot yielded an apparent K_m of 9.5 μM, which is in excellent agreement with the previously published value of 9.6 μM (6). The value we obtained for V_{max} is 0.65 s^{-1}, which is slower than k_1 and k_2 but is clearly faster than k_3 under similar experimental conditions (see Fig. 4). The observation that V_{max} is actually faster than k_3 (0.3 s^{-1}) leads us to conclude that k_3 represents a minor parallel reaction pathway or is eliminated when DsbA is present in excess. If k_3 were rate-limiting, then it would be impossible to reach a steady-state reaction rate higher than 0.3 s^{-1}. Thus k_2, which reflects the rate of quinone reduction, is likely to be the overall rate-limiting step. Why then is V_{max} significantly slower than k_2 (2 s^{-1})? In multiple turnover experiments, we are forced to use excess Q1 (because of the insoluble nature of Q8), and as discussed previously, Q1 is a nonideal cofactor that is reduced more slowly by DsbB compared with the rate of Q8 reduction. Indeed, in single turnover experiments using Q1, the quinone reduction step (as measured by absorbance decay at 510 and 275 nm; see Fig. 7) is closer to the measured V_{max} of 0.65 s^{-1}.

Stopped Flow Absorbance Measurement with DsbB Bearing a Menaquinone Cofactor—We have presented evidence that quinone reduction is the rate-limiting step in the DsbB reaction cycle, and that this step is preceded by a rapid intramolecular thiol-disulfide exchange reaction. If quinone reduction is truly rate-limiting, then substituting the Q8 cofactor of DsbB with quinones of different redox potentials should selectively affect the rate of this step. If, on the other hand, there is a rate-limiting step that precedes quinone reduction (such as a conformational change or thiol-disulfide exchange reaction), then the rate of quinone reduction should not depend on the redox potential of the quinone cofactor. This phenomenon has been observed previously in photosynthetic reaction centers (30), which led to the coining of the term "conformational gating." This implies that there is a step other than charge transfer (such as a conformational change) that "gates" the flow of electrons.

To test for the possibility of conformational gating within DsbB, and to further test our hypothesis that quinone reduction is rate-limiting, we performed stopped flow absorbance measurements of the reaction of menaquinone-bound DsbB, designated DsbB(MK), with DsbA. Menaquinone has a standard redox potential of −67 mV (31), compared with +113 mV for ubiquinone (22). Because menaquinone is less oxidizing than ubiquinone, we expected that DsbB would reduce menaquinone more slowly than ubiquinone (Q8) unless there were some other rate-limiting step(s) preceding quinone reduction. As shown in Fig. 10, this is precisely what is observed with DsbB(MK). Upon mixing with DsbA, there is a rapid increase in absorbance, the rate of which (~10 s^{-1}) is very similar to that observed when mixing DsbB(UQ) with DsbA under similar conditions and protein concentrations. This underscores the idea that the nature of the quinone does not affect DsbA binding or the subsequent thiol-disulfide exchange event. The rate

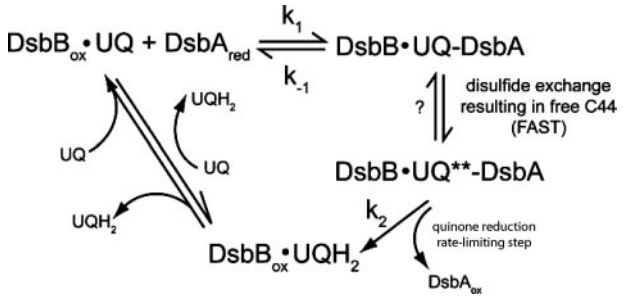

SCHEME 1. **Kinetic scheme for the DsbB reaction cycle.** See "Discussion."

of absorbance decay (which presumably reflects the rate of quinone reduction), on the other hand, is decreased from 2 s^{-1} for DsbB(UQ) to 0.3 s^{-1} for DsbB(MK). The observation that the rate of quinone reduction (as monitored by decay at 510 nm) is dependent on the redox potential of the quinone cofactor provides further evidence that quinone reduction is rate-limiting in the overall reaction cycle. Interestingly, the rate of menaquinone reduction is very similar to the rate of the second (minor) decay phase (k_3) observed in experiments carried out with DsbB(UQ). It is tempting to speculate that the reason for the presence of this phase observed with DsbB(UQ), and indeed the presence of a "fast" and "slow" reaction pathway in general, is simply because of a small fraction of DsbB containing a quinone (such as menaquinone) other than ubiquinone Q8.

Conclusions—We have studied the kinetics of the DsbB reaction cycle in detail. Our results support a kinetic model for DsbB (Scheme 1) in which DsbA binding is followed by a very rapid thiol-disulfide exchange reaction. This results in the free thiolate of Cys^{44} and the appearance of the Cys^{44}-UQ charge-transfer intermediate. This rapid exchange following DsbA binding could effectively prevent the unproductive back reaction of reduced DsbA dissociation, which occurs at a much slower rate. This also allows DsbA binding to be tightly coupled to quinone reduction. Quinone reduction appears to be the rate-limiting step in the overall reaction cycle. This is supported by the observation that substitutions of the quinone cofactor selectively affected the rate of quinone reduction, whereas the steps leading up to quinone reduction were unchanged. The mechanism of quinone recycling/exchange was not addressed in the present work, and this remains an important and interesting issue to resolve to further expand our understanding of this complex enzyme. These studies set the stage for addressing the mechanism of quinone recycling or exchange to regenerate a catalytically competent DsbB.

Acknowledgments—We thank Ursula Jakob and Jonathan Pan for critical evaluation of the manuscript. We also thank Dave Arscott for helpful discussions and John Hsieh for technical assistance.

REFERENCES

1. Kadokura, H., Katzen, F., and Beckwith, J. (2003) *Annu. Rev. Biochem.* **72,** 111–135
2. Nakamoto, H., and Bardwell, J. C. (2004) *Biochim. Biophys. Acta* **1694,** 111–119
3. Frech, C., Wunderlich, M., Glockshuber, R., and Schmid, F. X. (1996) *EMBO J.* **15,** 392–398
4. Zapun, A., and Creighton, T. E. (1994) *Biochemistry* **33,** 5202–5211
5. Bader, M., Muse, W., Ballou, D. P., Gassner, C., and Bardwell, J. C. (1999) *Cell* **98,** 217–227
6. Bader, M., Muse, W., Zander, T., and Bardwell, J. (1998) *J. Biol. Chem.* **273,** 10302–10307
7. Bader, M. W., Xie, T., Yu, C. A., and Bardwell, J. C. (2000) *J. Biol. Chem.* **275,** 26082–26088
8. Kobayashi, T., and Ito, K. (1999) *EMBO J.* **18,** 1192–1198
9. Kobayashi, T., Kishigami, S., Sone, M., Inokuchi, H., Mogi, T., and Ito, K. (1997) *Proc. Natl. Acad. Sci. U. S. A.* **94,** 11857–11862
10. Regeimbal, J., Gleiter, S., Trumpower, B. L., Yu, C. A., Diwakar, M., Ballou, D. P., and Bardwell, J. C. (2003) *Proc. Natl. Acad. Sci. U. S. A.* **100,** 13779–13784
11. Inaba, K., Takahashi, Y. H., Fujieda, N., Kano, K., Miyoshi, H., and Ito, K. (2004) *J. Biol. Chem.* **279,** 6761–6768
12. Inaba, K., Takahashi, Y. H., Ito, K., and Hayashi, S. (2006) *Proc. Natl. Acad. Sci. U. S. A.* **103,** 287–292
13. Zapun, A., Bardwell, J. C., and Creighton, T. E. (1993) *Biochemistry* **32,** 5083–5092
14. Guilhot, C., Jander, G., Martin, N. L., and Beckwith, J. (1995) *Proc. Natl. Acad. Sci. U. S. A.* **92,** 9895–9899
15. Kishigami, S., and Ito, K. (1996) *Genes Cells* **1,** 201–208
16. Kishigami, S., Kanaya, E., Kikuchi, M., and Ito, K. (1995) *J. Biol. Chem.* **270,** 17072–17074
17. Grauschopf, U., Fritz, A., and Glockshuber, R. (2003) *EMBO J.* **22,** 3503–3513
18. Inaba, K., and Ito, K. (2002) *EMBO J.* **21,** 2646–2654
19. Inaba, K., Takahashi, Y. H., and Ito, K. (2005) *J. Biol. Chem.* **280,** 33035–33044
20. Regeimbal, J., and Bardwell, J. C. (2002) *J. Biol. Chem.* **277,** 32706–32713
21. Xie, T., Yu, L., Bader, M. W., Bardwell, J. C., and Yu, C. A. (2002) *J. Biol. Chem.* **277,** 1649–1652
22. Gennis, R. B., and Stewart, V. (1996) in *Escherichia coli and Salmonella, Cellular and Molecular Biology* (Neidhardt, F. C., ed) p. 222, American Society for Microbiology, Washington, D. C.
23. Urban, P. F., and Klingenberg, M. (1969) *Eur. J. Biochem.* **9,** 519–525
24. Inaba, K., Murakami, S., Suzuki, M., Nakagawa, A., Yamashita, E., Okada, K., and Ito, K. (2006) *Cell* **127,** 789–801
25. Takahashi, Y. H., Inaba, K., and Ito, K. (2004) *J. Biol. Chem.* **279,** 47057–47065
26. Riddles, P. W., Blakeley, R. L., and Zerner, B. (1979) *Anal. Biochem.* **94,** 75–81
27. Gibson, Q. H., Swoboda, B. E., and Massey, V. (1964) *J. Biol. Chem.* **239,** 3927–3934
28. Hennecke, J., Sillen, A., Huber-Wunderlich, M., Engelborghs, Y., and Glockshuber, R. (1997) *Biochemistry* **36,** 6391–6400
29. Kadokura, H., and Beckwith, J. (2002) *EMBO J.* **21,** 2354–2363
30. Graige, M. S., Feher, G., and Okamura, M. Y. (1998) *Proc. Natl. Acad. Sci. U. S. A.* **95,** 11679–11684
31. Wagner, G. C., Kassner, R. J., and Kamen, M. D. (1974) *Proc. Natl. Acad. Sci. U. S. A.* **71,** 253–256